Surface Science 233 (1990) 248–254
North-Holland

RELAXATIONS IN THE MISSING-ROW STRUCTURE OF THE (1 × 2) RECONSTRUCTED SURFACES OF Au(110) AND Pt(110)

E. VLIEG, I.K. ROBINSON

AT&T Bell Laboratories, Murray Hill, NJ 07974, USA

and

K. KERN

AT&T Bell Laboratories, Murray Hill, NJ 07974, USA
and
IGV-KFA Jülich, D-5170 Jülich, Fed. Rep. of Germany

Received 19 December 1989; accepted for publication 8 March 1990

The atomic structure of the (1 × 2) reconstructed (110) surfaces of Au and Pt has been investigated in detail using X-ray diffraction. For both surfaces the reconstruction involves several layers of atoms. The top layer spacing is contracted and pairing occurs in the second and fourth layers.

There have been enough investigations of these surfaces with other experimental methods that a detailed comparison can now be made. Though there is full agreement on the missing-row model, this is not true for the magnitude of the relaxations occurring at the surfaces. In general the X-ray diffraction results compare better with electron diffraction data than with ion scattering experiments. Many theoretical approaches fail to predict the correct sign and/or magnitude of some of the relaxations.

1. Introduction

The phenomenon of spontaneous reconstructions of metal surfaces and understanding its origin has for long been a strong motivation in surface science. The structure of the (1 × 2) reconstructed (110) faces of Au, Pt and Ir has been the subject of a great number of experimental [1–12] and theoretical [13–17] papers. Of these three systems Au(110) has attained most experimental attention [1–6], while detailed experiments on Pt(110) have been done only more recently [8–10]. Data on Ir(110) is relatively scarce [11,12].

By now, the missing-row model (see fig. 1) for the structure of the (1 × 2) reconstructed surface is well established, and attention has shifted to relaxations occurring at the surface. The initial low-energy electron diffraction (LEED) experiment [1] indicated a contraction of the top-layer spacing for Au. In contrast, an early surface X-ray diffraction study [2], and a high-resolution electron microscopy study [3], pointed to an expansion of the top-layer spacing. All later experiments, however, using LEED [4], low-energy ion scattering (LEIS) [5] and medium-energy ion scattering (MEIS) [6] provided strong evidence for a contraction of the top-layer spacing. A new electron-microscopy study [18] also claimed a contraction, leaving X-ray diffraction the only technique still claiming an expansion.

Since the early experiment on Au(110), X-ray diffraction has been used to investigate a great number of surface structures and has become a valuable tool in surface science [19,20]. Considerable advances in the technique have taken place and much confidence has been gained in the interpretation of crystallographic data. Bearing this in mind and considering the continued interest in the details of the structure, it seemed appropriate to reinvestigate the structure of Au(110)-(1 × 2).

In addition to relaxation of the layer spacings, also a pairing in the second layer (see fig. 3) has

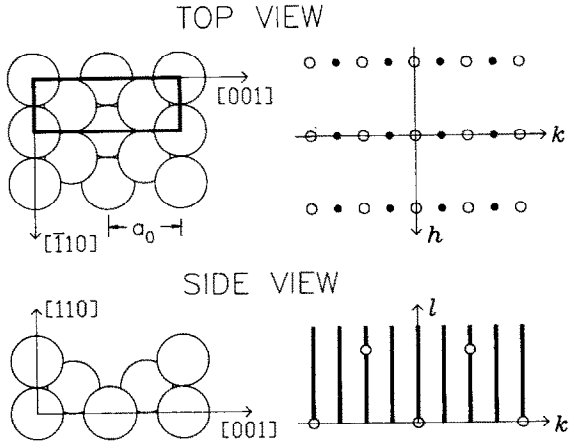

Fig. 1. Schematic of the missing row surface unit cell (left) and the corresponding reciprocal lattice (right), with the crystallographic directions indicated. In the top view open circles represent integer-order reflections and filled circles are half-order reflections, which contain information of the reconstructed surface only. Due to the two-dimensional character of the surface, the intensity is continuous along the l (perpendicular) direction. The circles are bulk Bragg peaks within the integer-order rods.

been found in X-ray diffraction [2] and LEED [3] experiments, but not by MEIS [6]. Theoretical calculations [13–16] and LEED experiments on the related Pt(110)-(1 × 2) system [8,9] suggest that also deeper layers may show lateral displacements. This is therefore also considered in the present analysis. Accurate values of the relaxations allow an evaluation of the validity of the various theoretical approaches that have been used to calculate the relaxed Au(110)-(1 × 2) surface structure.

The Pt(110)-(1 × 2) system has not been studied by X-ray diffraction before. The first LEED study [7] on this system favored an expansion of the top-layer spacing, but all further experiments agreed on a contraction [8–10]. Whereas LEED [8,9] found significant pairing in the second and fourth layers, as it does in the case for Au, MEIS [10] does not find any such evidence. These issues are also examined in the present study.

2. Experiment

The experiments were performed at beam line X16A at the National Synchrotron Light Source (NSLS) at Brookhaven National Laboratory. 5 milliradians of radiation were focused by a toroidal Pt-coated mirror at 5.7 milliradians angle of incidence. The X-ray beam was monochromated by two parallel Si(111) crystals to a wavelength of 1.09 Å. The samples were mounted in an ultra-high-vacuum (UHV) chamber coupled to a 4-circle diffractometer [21]. The whole set-up could be rotated on a vertical axis, providing a fifth degree of freedom.

The Au surface was prepared by Ar sputtering, followed by a 450°C anneal. The initial surface preparation of the Pt crystal required extensive annealing cycles in O_2 (1×10^{-7} mbar, 700°C) and H_2 (5×10^{-7} mbar, 900°C), in order to remove C and S. After that, the surface was sputtered (1×10^{-5} mbar Ar, 500°C) to remove Ca and Si, followed by a 900°C anneal. This also had to be repeated several times. The surface cleanliness of the crystals was checked by Auger-electron spectroscopy. After extended annealing, Sn could always be detected on the Au sample. However, the present measurements were done at room temperature, and no contaminants were observable at the prepared surfaces. Unlike another recent study on Au(110) [22], we never found any evidence for a 1 × 3 reconstruction on that surface.

The illuminated surface area was determined by 2 mm slits on the incoming beam and 2 mm slits on the exit beam. This led to a sin 2θ dependence in the area, for which the data had to be normalized [19,23]. For very small 2θ angles, the area defined by the slits became larger than the sample size, and an additional correction was necessary. The fifth degree of freedom allowed the surface normal to be set horizontal for all scans [24]. This geometry considerably simplified the normalization of the data, because no corrections were necessary for the tilt-dependence in the illuminated surface area, nor for changes in the resolution function arising from the tilt of the diffraction rods [23].

The sample surfaces were aligned using a laser beam. The crystallographic alignment was done by determining the position of two out-of-plane bulk reflections. For convenience a surface unit cell was employed following the LEED convention [25]. The surface lattice vectors can be expressed in

terms of the conventional cubic lattice vectors by $\boldsymbol{a}_1 = \frac{1}{2}(\bar{1}10)_{cub}$; $\boldsymbol{a}_2 = (001)_{cub}$; $\boldsymbol{a}_3 = \frac{1}{2}(110)_{cub}$. The component of the momentum transfer perpendicular to the surface is then represented by the single Miller index l. This coordinate frame is also explained in fig. 1.

For small values of l, the angle of incidence and the outgoing angle were set equal. For larger l values, the outgoing angle was fixed at 3°, which reduced somewhat the observed thermal diffuse background from the bulk. The angles were always well above the critical angle for total reflection (about 0.4°), so that no refraction effects occurred. Scans across the fractional order rods were made by rotating the ϕ axis of the diffractometer. The integrated intensity was determined by numerically integrating the peak and subtracting the background as determined from the intensity far away from the peak. These integrated intensities were corrected for the illuminated surface area and Lorentz factor. Taking the square root gave the experimental structure factor.

For both surfaces, a large number of (hk) reflections were measured for various values l of momentum transfer along the diffraction rods (see fig. 1). Data with non-zero l values gave information on relaxations perpendicular to the surface. The error in the data was estimated by combining the measured variation between symmetry-equivalent reflections with the error due to counting statistics [19]. The first contribution generally dominated the total error. On the Au(110) sample, a total of 141 non-equivalent reflections were measured, corresponding to 23 different (hk) rods sampled at a number of l values. On the Pt(110) sample the data set consisted of 88 reflections from 23 different (hk) rods.

Representative rod scans are shown in fig. 2. It is clear that the rod profiles of Au(110) and Pt(110) are very similar, indicating that the reconstructed surfaces have the same structure. The rapid modulation of the measured profiles shows immediately that the reconstruction involves more than one layer of atoms. The experimental measurements of the (0, 1.5) and (0, 2.5) rod profiles for Au(110) are in good agreement with the earlier work [2]. At that time the rapid modulation was

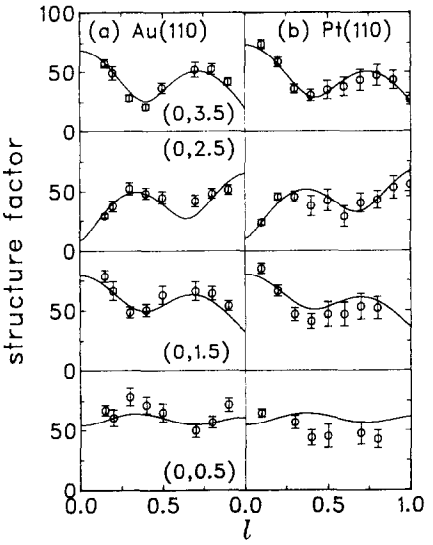

Fig. 2. The structure factors of several (hk) reflections as a function of the perpendicular momentum transfer l for Au(110) and Pt(110). The circles are the data points, the solid curves are the best fits to the data.

thought to come from (and agreed with) a two layer structure with an enlarged layer spacing. The wider range of current data is inconsistent with this interpretation and necessitate a more complex model with displacements in a greater number of layers.

The measured structure factors were fitted using a χ^2 minimization, starting from the missing-row model and allowing the atom positions to move in directions according to the Pmm2 symmetry of the unit cell (fig. 3). The fitted parameters in the case of Au were a vertical displacement of atom layer

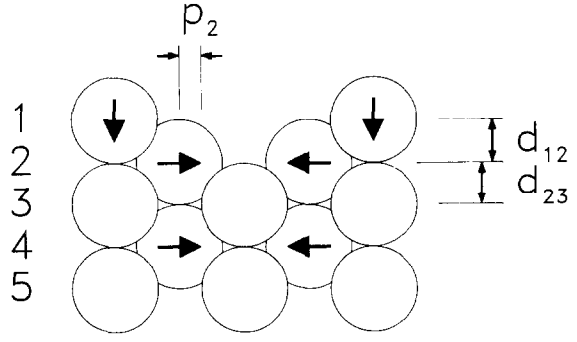

Fig. 3. Definition of the various relaxation parameters in the missing-row structure of the (1×2) reconstructed surfaces of Au(110) and Pt(110).

Table 1
Summary of the optimum values for the fitting parameters for Au and Pt

	Au(110)	Pt(110)
Δd_{12}	-0.32 ± 0.10	-0.27 ± 0.10
Δd_{23}	–	-0.11 ± 0.08
p_2	0.05 ± 0.01	0.05 ± 0.01
p_4	0.05 ± 0.01	0.04 ± 0.01
B_1	1.5 ± 0.1	0.9 ± 0.1
B_2	1.4 ± 0.3	1.0 ± 0.2
B_4	0.8 ± 0.2	(0.29)
χ^2	2.6	2.1

Δd is the change in layer spacing (Å), p represents pairing (Å), see fig. 3. The Debye–Waller parameters B are expressed in Å^2.

1, pairing of layers 2 and 4, and the Debye-Waller parameters of layers 1, 2 and 4. The optimal values for these fitting parameters are given in table 1, the calculated rod profiles are shown as the solid curves in fig. 2a. The fit has a χ^2 value of 2.6, which should be compared with the value of 7.9 for the missing-row model without relaxations. The rather large value of χ^2 is likely to be caused by the uncertainties in the estimation of the errors in the data points. Due to the limited range in l, the data are insensitive to vertical relaxations and/or buckling in layers beyond the first. Including a pairing in the sixth layer did not improve the fit further. The data are very sensitive to such lateral displacements, so the occurrence of a significant pairing in that layer seems unlikely. The optimized isotropic Debye–Waller parameters of layers 1 and 2 correspond to a mean thermal vibration amplitude of 0.14 Å, which is a significant enhancement over the bulk value of 0.088 Å.

The analysis of the Pt(110)-(1 × 2) data was completely analogous. The results of the fitting are shown in table 1 and in fig. 2b. In this case the vertical displacement of the second layer was also optimized, because it gave a significant improvement in the fit. Again the surface atoms show an enhanced thermal vibration amplitude. A Debye–Waller parameter of 1 corresponds to a mean vibration amplitude of 0.11 Å, which should be compared with the bulk value of 0.061 Å.

3. Discussion

In table 2 the present results for Au(110)-(1 × 2) are compared with other measurements and several recent theoretical calculations. In the present analysis we found a contraction of the top-layer spacing, in excellent agreement with all recent measurements. As noted above, the top-layer expansion as found in the earlier X-ray diffraction study [2], was caused by the limited out-of-plane data set which could be described by a simple two-layer

Table 2
A summary of the most relevant work on Au(110)-(1 × 2)

		Δd_{12}	Δd_{23}	p_2	p_4	b_3
Experiments						
X-ray diffraction	This work	−0.32	–	0.05	0.05	–
X-ray diffraction	[2]	0.62	–	0.12	–	–
LEED	[4]	−0.29	0.03	0.07	–	0.24
LEIS	[5]	−0.20	–	< 0.1	–	–
MEIS	[6]	−0.26	0.06	< 0.1	–	0.20
Theories						
Tight-binding	[13]	−0.09	0.03	0.02	–	–
Tight-binding	[17]	−0.16	−0.04	−0.08	0.07	0.11
"Glue"-model	[14]	−0.39	−0.09	−0.27	0.12	0.40
Embedded atom	[15]	−0.21	−0.07	−0.04	0.04	0.11
First principles	[16]	−0.23	0.03	0.05	0.09	0.20

All displacements are given in Å. The meaning of the Δd's and p's is explained in fig. 3. b_3 represents buckling in the third layer, with a positive value meaning an upward displacement of third-layer atoms without a first-layer atom on top.

model. The fact that pairing in the fourth layer was disregarded, also gave a larger estimate of the second layer pairing in ref. [2] than found here. The LEED analysis [4] found a value for the pairing in the second layer in close agreement with the value obtained here. The MEIS data [6] did not show any evidence for such pairing. The present data give the first evidence for pairing in the fourth layer of Au(110)-(1 × 2).

Comparing the results of the various theoretical methods shown in table 2 with the available data, we see that all methods predict a contraction of the top-layer spacing, but with a large variation in the estimated values. The embedded-atom method [15] and a first-principles calculation [16] give values that are closest to the average experimental value. The first-principles calculation predicts in addition the correct sign and magnitude of the second-layer pairing. The embedded-atom method predicts the wrong direction of the second-layer displacement. The "glue" model [14] shows a tendency to overestimate the relaxations at the surface and in particular gives a bad estimate of the second layer pairing. The two tight-binding calculations [13,17] have poor agreement with each other and with the data.

The enhancement of the mean thermal vibration amplitude by a factor ~ 1.5 as found here is the same as obtained in the older X-ray diffraction analysis [2], and also agrees well with ion scattering results [6,26]. In the LEED analysis [4], no surface-enhanced thermal vibration was taken into account. Simple model calculations [27] indicated anisotropic behavior at the (110) surface: no significant enhancement was predicted along the close-packed [$\bar{1}$10] direction, but along the [110] and [001] directions the enhancement was calculated to be a factor ~ 1.5. In the data analysis, we employed isotropic Debye–Waller parameters, because the introduction of anisotropy did not lead to significantly improved fits. Though none of the studies mentioned here claim a high accuracy, all point to an enhancement of the mean thermal vibration amplitude at the surface by a factor ~ 1.5.

In table 3 a comparison is made between the various results on Pt(110)-(1 × 2). There is an excellent agreement between the experimental values obtained for the contraction of the first layer spacing. The agreement is less strong on the second to third layer spacing. Both X-ray diffraction and LEED agree on a second-layer pairing of ~ 0.05 Å. Surprisingly, the ion scattering results indicate that no pairing occurs at all. This may arise because ion scattering measures an atomic alignment angle in the crystal, which is therefore sensitive to both parallel and perpendicular displacements and cannot readily distinguish between them. Or else it may be related to uncertainties in the estimate of the thermal vibration amplitudes at the surface and the degree to which these are correlated. The value found here for the fourth-layer pairing of 0.04 Å agrees well with one LEED analysis that found 0.05 Å [9], but not with the other, that derived a pairing of 0.12 Å [8].

The two theoretical calculations give results similar to the case of Au. The tight-binding scheme [13] gives too small relaxations, whereas the em-

Table 3
A summary of the most relevant work on Pt(110)-(1 × 2)

		Δd_{12}	Δd_{23}	p_2	p_4	b_3
Experiments						
X-ray diffraction	This work	−0.27	−0.11	0.05	0.04	–
LEED	[8]	−0.26	−0.18	0.07	0.12	0.32
LEED	[9]	−0.28	−0.01	0.04	0.05	0.17
MEIS	[10]	−0.22	0.06	< 0.04	–	0.10
Theories						
Tight-binding	[13]	−0.11	0.02	0.02	–	–
Embedded atom	[15]	−0.25	−0.07	−0.03	0.04	0.11

See footnote to table 2 for an explanation.

bedded-atom method [15] again gives an excellent prediction for the top-layer spacing, but calculates the wrong sign for the second layer pairing.

The enhancement of the thermal vibration amplitude by a factor of ~ 1.4 is again in reasonable agreement with ion scattering data [10] and model calculations [27]. LEED analyses have derived enhancement factors of 2.2 [28] and 1.4 [8], or have ignored surface enhancements [9].

4. LEED versus X-ray diffraction

Au(110) and Pt(110) are among the best studied surface structures to date, with state-of-the-art LEED and X-ray results to compare. We would like to take this opportunity to reflect a little on the relative accuracy of determination of the various parameters with the aid of fig. 4. The agreed-upon missing-row structure is relatively simple and has important structural parameters both parallel and perpendicular to the plane. It also displays simultaneously three contrasting modes of reconstruction: density modification (top layer), pairing (2nd and 4th layers) and buckling (3rd layer). Fig. 4 shows a side view of reciprocal space with rods representing the desired data in an ideal diffraction experiment (LEED or X-ray). A cutoff hemisphere is drawn to indicate some desired resolution limit: a complete, accurate set of measurements inside the sphere of radius q_{max} would allow the structure to be determined to an error of order 5% of $2\pi/q_{max}$ due to series termination effects [29] and depending somewhat on the accuracy of the data. This error would be isotropic. However, neither technique can measure the full hemisphere; a typical range of data is shown in the figure for LEED, four-circle [30] and five-circle [24] surface X-ray diffractometers.

LEED is primarily a backscattering technique, probing mainly perpendicular momentum transfer (fig. 4a). It is particularly sensitive to vertical displacements. It was able to detect 3rd layer buckling both in Au(110) and Pt(110), which was beyond the level of significance of the X-ray data. Though no error bars are shown, perpendicular distances from LEED are accurate in tables 2 and 3; parallel ones are less so.

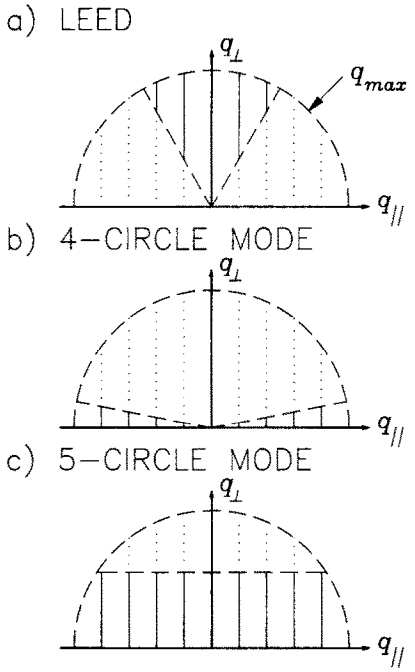

Fig. 4. Schematic reciprocal space diagrams showing the limited range of diffraction data available to different techniques. The rods represent data. q is the momentum transfer for which $q_{\parallel}$ and $q_{\perp}$ are the respective components. The hemispherical diffraction limit is an arbitrary total resolution cutoff at $|q| = q_{max}$. (a) Low-energy electron diffraction (LEED). The cone angle in reciprocal space equals half the total scattering angle accepted by the screen (120° here). LEED system designs might vary slightly but will not affect this picture dramatically. (b) Four-circle X-ray diffraction [30]. Here the cone angle is given by the maximum tilt angle accessible to the sample, limited by feedthroughs etc. (11° here [21]). The same tilting limitations and diagram apply to transmission electron diffraction (TED). (c) Five-circle X-ray diffraction [24] or X-ray diffraction with out-of-plane detector arm [20]. The limiting perpendicular limit is given by the wave vector times the sine of the maximum inclination angle (about 20° for the diffractometer used [21]).

Conversely, X-ray diffraction as most commonly practiced is a grazing angle technique, with a correspondingly different subset (fig. 4b) of the data sampled. The four-circle (sample tilting) geometry [30] is particularly restrictive. The small range of data for the old Au(110) study [2] led to a model with a top layer expansion as discussed above.

The extension to the five-circle mode [24] has improved the situation significantly, as fig. 4c

shows. The incident beam can be inclined to a large angle relative to the surface, improving the range of perpendicular momentum transfer. This is analogous to moving the detector out of plane [20]; the ability to do both is an anticipated further improvement. This was the geometry used in the present study. Parameters for Au(110) and Pt(110) in table 1 are still better determined in-plane than out-of plane, but we have sufficient vertical information to avoid ambiguity in this and most other cases. More perpendicular data range is needed to determine reliably the small (1–5%) layer spacing relaxations seen in many otherwise unreconstructed surfaces. LEED is probably still the best technique for this because of its great vertical sensitivity.

5. Conclusions

Using extensive data sets including reflections with non-zero perpendicular momentum transfer, various relaxations in the missing-row structure of Au(110)-(1 × 2) and Pt(110)-(1 × 2) have been determined. The top-layer spacing is contracted and pairing occurs in the second and fourth layers. All recent experiments agree on the top-layer contraction. The discrepancy with an earlier X-ray diffraction study, which found a top-layer expansion, is explained. The pairing in the second layer is in agreement with LEED experiments, but less so with ion-scattering results. Of all theoretical methods used to calculate the relaxations at the surface, only a first-principles calculation agrees with the experimental results.

Acknowledgments

We would like to thank B.A. Frenz for the continuous support of the "Personal SDP" crystallographic software package that was used to analyze the data, and A.A. Macdowell for his assistance during the measurements. We thank T. Gustafsson for a critical reading of the manuscript. NSLS is supported by the United States Department of Energy under contract DE-AC02-76CH00016.

References

[1] W. Moritz and D. Wolf, Surf. Sci. 88 (1979) L29.
[2] I.K. Robinson, Phys. Rev. Lett. 50 (1983) 1145.
[3] L.D. Marks, Phys. Rev. Lett. 51 (1983) 1000.
[4] W. Moritz and D. Wolf, Surf. Sci. 163 (1985) L655.
[5] J. Möller, K.J. Snowdon, W. Heiland and H. Niehus, Surf. Sci. 178 (1986) 475;
H. Derks, H. Hemme, W. Heiland and S.H. Overbury, Nucl. Instrum. Methods B 23 (1987) 374.
[6] M. Copel and T. Gustafsson, Phys. Rev. Lett. 57 (1986) 723.
[7] D.L. Adams, H.B. Nielsen, M.A. Van Hove and A. Ignatiev, Surf. Sci. 104 (1981) 47.
[8] E.C. Sowa, M.A. Van Hove and D.L. Adams, Surf. Sci. 199 (1988) 174.
[9] P. Fery, W. Moritz and D. Wolf, Phys. Rev. B 38 (1988) 7275.
[10] P. Fenter and T. Gustafsson, Phys. Rev. B 38 (1988) 10197.
[11] C.-M. Chan and M.A. Van Hove, Surf. Sci. 171 (1986) 226.
[12] W. Hetterich and W. Heiland, Surf. Sci. 210 (1989) 129.
[13] H.-J. Brocksch and K.H. Bennemann, Surf. Sci. 161 (1985) 321.
[14] M. Garofalo, E. Tosatti and F. Ercolessi, Surf. Sci. 188 (1987) 321.
[15] S.M. Foiles, Surf. Sci. 191 (1987) L779.
[16] K.-M. Ho and K.P. Bohnen, Europhys. Lett. 4 (1987) 345; Phys. Rev. Lett. 59 (1987) 1833.
[17] M. Guillop and B. Legrand, Surf. Sci. 215 (1989) 577.
[18] T. Hasegawa, N. Ikarashi, K. Kobayashi, K. Takayanagi and K. Yagi, in: The Structure of Surfaces II, Eds. J.F. van der Veen and M.A. Van Hove (Springer, Berlin, 1988) p. 43.
[19] I.K. Robinson, in: Handbook on Synchrotron Radiation, Vol. 3, Eds. D. Moncton and G. Brown (North-Holland, Amsterdam, in preparation).
[20] R. Feidenhans'l, Surf. Sci. Rep. 10 (1989) 105.
[21] P.H. Fuoss and I.K. Robinson, Nucl. Instrum. Methods 222 (1984) 171.
[22] G.A. Held, J.L. Jordan-Sweet, P.M. Horn, A. Mak and R.J. Birgenau, Solid State Commun. 72 (1989) 37.
[23] I.K. Robinson, Aust. J. Phys. 41 (1988) 359.
[24] E. Vlieg, J.F. van der Veen, J.E. Macdonald and M. Miller, J. Appl. Cryst. 20 (1987) 330.
[25] See for example: F. Jona, J.A. Strozier and W.S. Wang, Rep. Prog. Phys. 45 (1982) 527.
[26] H. Derks, J. Möller and W. Heiland, Surf. Sci. 188 (1987) L685.
[27] D.P. Jackson, Surf. Sci. 43 (1974) 431.
[28] H.B. Lyon and G.A. Somorjai, J. Chem Phys. 44 (1966) 3707.
[29] H. Lipson and W. Cochran, The Determination of Crystal Structures, 3rd ed. (Cornell University Press, Ithaca, NY, 1966) ch. 12, pp. 317–357.
[30] I.K. Robinson, Rev. Sci. Instrum. 60 (1989) 1541.